# MCCI IN AN HOMOGENEOUS POOL: LESSONS LEARNT FROM MCCI-OECD AND VULCANO REAL MATERIAL EXPERIMENTS IN DRY CONDITIONS

Authors: M. Cranga, C. Mun, C. Marchetto
Institut de Radioprotection et de Sûreté Nucléaire, IRSN, DPAM, SEMIC
13115 St Paul Lez Durance, France
Tél. : +(33) 4 42 19 94 82, Fax : +(33) 4 42 19 91 67, E-mail : michel.cranga@irsn.fr

This work updates and completes the study presented at the last MCCI seminar in 2007 [1]. The purpose of the present work is to present an interpretation of outstanding 2D MCCI tests in an homogeneous corium pool configuration in dry conditions, from the OECD-MCCI [2,3,4] and the VULCANO [5,6] programs.

This interpretation has been performed with the help of the MEDICIS module of ASTEC calculation code [7], developed by IRSN in collaboration with the German GRS organisation. More precisely, this analysis is focussed on tests CCI2, CCI3 and CCI5 on one hand, and VBU5/VBES-U2 on the other hand, in order to improve the understanding of the 2D ablation behaviour.

## 1 General approach

General modelling assumptions used for these interpretations are presented below. The models have been developed in the ASTEC/MEDICIS code [7] that computes the MCCI processes in case of severe accidents mainly for PWR plants. ASTEC is coupled with GEMINI2 code using the NUCLEA 09 database [8] to obtain the necessary thermo-chemistry data, mainly for MCCI the corium mass and volume liquid fraction versus the temperature. Capability of ASTEC to easily integrate new models makes it also a suitable tool to build scenarios explaining small scale experiment results.

The convective heat transfer towards the corium/concrete interface is evaluated from a correlation fitted on Bali data [9]. In present calculations, the corium physical properties and in particular the viscosity impacting on the convective heat transfer coefficient are evaluated at the pool bulk temperature: this means in particular that the viscosity gradient near the pool/concrete interface is ignored in the present approach.

It is recalled that no experimental proof of a stable crust at concrete/corium interface can be derived from most available post-test examinations (PTE) of real material MCCI experiments, whatever the concrete type. Besides, the crust observed at the pool/concrete interface only in PTE of VBU7 test is an indication of an initial build-up of crust but this crust might stay then inert without further growth due to corium solidification later during the test. Therefore, a new simplified approach is proposed here, assuming a mushy boundary layer without a stable crust all along pool/concrete interfaces and without link with corium solidification. The heat transfer from the bulk pool to the concrete interface is determined only by convection in the bulk, and the heat transfer at the concrete interface, whose thermal resistance depends on the interface orientation, is imposed using the hslag heat transfer coefficient in the slag layer. This simplified modelling is represented on figure 1.

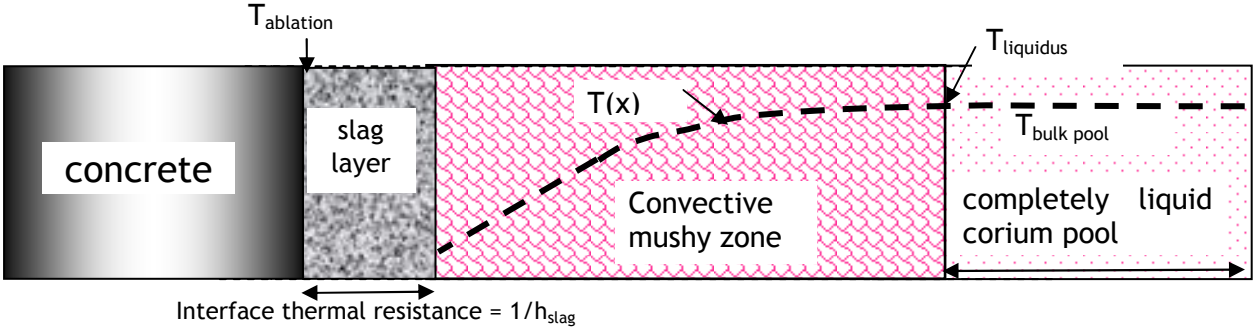


**Figure 1: Pool/concrete interface structure**

Since the thermodynamic equilibrium at the bulk pool/upper crust interface is likely not reached in real material experiments because of transient conditions, high gas bubbling and high liquid corium viscosity due to the presence of ablated concrete species (silica…), the upper crust is assumed to be in a mushy state. The uncertainty concerns the evaluation of the inner temperature of this boundary layer, usually called 'solidification temperature'. In the former approach presented in 2007 [1], this temperature was determined from liquidus and solidus temperature using the expression:

$$T_{solidif} = \gamma.T_{solidus} + (1-\gamma).T_{liquidus}$$

where the $\gamma$ interpolation parameter stands between 0.2 and 0.4. However, based on experimental observations, the upper crust thickness calculated was often largely overestimated using this type of assumption.

Hence this solidification interface temperature with the lower pool convective zone is now determined from a threshold volumetric solid fraction (around 50%) below which convective heat transfer is replaced by conduction and consequently is lower than the pool liquidus temperature. This modelling leads to a thinner and more realistic upper crust thickness (based on experimental data), when using a threshold value obtained by the software GEMINI2.

Other assumptions specifically taken due to the test conditions are presented and justified for each test interpretation in a dedicated section.

# 2 Interpretation of CCIX experiments

## *2.1 CCI2 test*

The CCI2 test [3] from the OECD-MCCI program is the first 2D MCCI real material experiment, with an homogeneous oxidic pool configuration, showing significant both lateral and axial ablations.

The correct slice geometry for the corium pool with only 2 ablatable lateral walls is described by MEDICIS. Conditions of the CCI2 test are deduced from the final data recommended after the CCI2 benchmark [10] and from updated data presented in the final MCCI program report [4]. The temperature of upper walls receiving the power radiated from the corium pool is assumed to be equal to the concrete ablation temperature. The very fast oxidation of initial Cr mass is supposed to be achieved at the MCCI onset. The initial corium composition takes into account an early corium splattering of 88 kg above the corium pool by a reduction of the initial corium inventory. The water injection is described, but its impact on the erosion kinetics remains small and is not analyzed below.

The concrete composition issued from benchmark recalculations [10] is very similar to that obtained from the final report [3], neglecting very minor species. The thermo-chemistry data are evaluated for the mixture of the initial corium inventory with increasing ablated concrete mass using an interface with the GEMINI2 solver and the NUCLEA database [8]. The value of the ablation temperature (1568K) and of the ablation enthalpy variation (2,38 MJ/kg) used by MEDICIS for evaluating the enthalpy of ablated oxide species at the ambient temperature coming into the pool are those recommended for CCI2 benchmark calculations [10].

### *2.1.1 Model assumptions*

For CCI2, it is assumed that no crust or solid accumulation is present along the concrete interface. The value of the heat transfer coefficient determining the thermal resistance of the concrete interface is taken independent of the interface orientation and equal to 300 $W/m^2/K$ as for the case of the lateral interface with siliceous concrete (see paragraph 2.2). The physical justification of this value is that the thermal resistance is generated by a mushy boundary layer including ablated concrete oxides and not by a more resistive crust or solid accumulation (see Discussion paragraph).

The solidification temperature determining the pool/upper crust interface temperature is evaluated from a volumetric solid fraction equal to 0.5 considered as typical of the transition in mushy state from a convective zone to a conductive one. In order to better estimate the observed high corium swelling; the corium void fraction is determined from the Zuber-Findlay correlation multiplied by a factor equal to 1.5, as this Zuber correlation might be not suitable for the MCCI situation involving specific phenomena such as foaming or a not established bubble flow regime.

### *2.1.2 CCI2 calculation results*

Results obtained are displayed for the axial and lateral ablation kinetics on figure 2, for the temperature evolution on figure 3 and for the cavity evolution on figure 4.

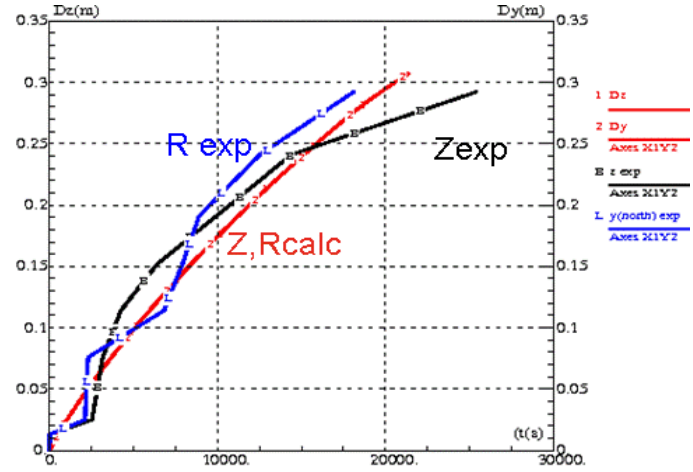


**Figure 2: axial (Z) and lateral (R) ablation kinetics.**

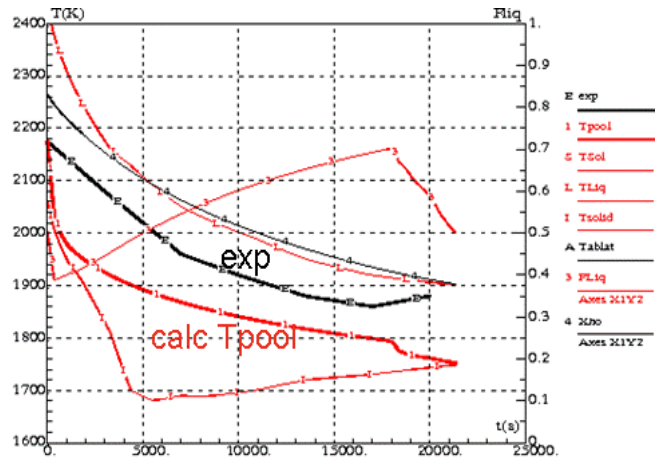


**Figure 3: pool temperature, solidification temp., mass liq. fraction, comparison with measured temperature.**

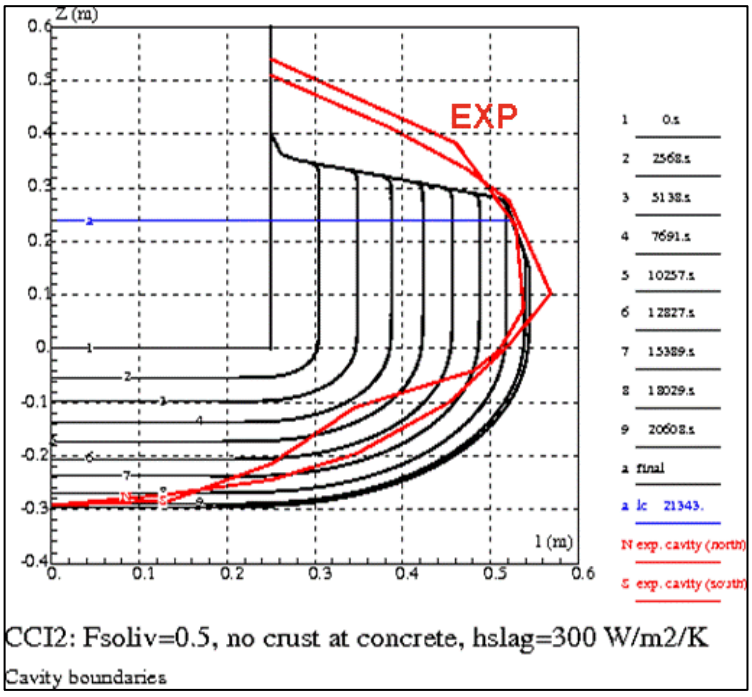


**Figure 4: cavity evolution, comparison with final experimental data (exp).**

The temperature is underestimated in the first phase by at most 160K and only by 80K in the late phase. Taking into account the simplistic assumptions used for describing the pool/concrete interface structure and the absence of model parameters fitting (threshold liquid fraction for evaluating the solidification temperature and slag layer heat transfer coefficient chosen as for other tests), the overall agreement between calculation and experiment is rather satisfactory. The underestimation of the upper cavity wall ablation might be due to the still too low calculated pool swelling. The final calculated ablated concrete mass is 350kg near the experimental value of 335.8kg, which shows that the assumptions lead to heat losses and corium composition close to those of the experiment.

## *2.2 CCI3 test*

At the opposite of CCI2, CCI3 test [3] using a siliceous concrete showed a large dissymmetry between the axial and lateral ablations.

### 2.2.1 *Conditions for CCI3 test*

Conditions of CCI3 test are deduced from the final experimental report [4]. Geometry and boundary conditions are very similar to those of CCI2 test. The temperature of upper walls receiving the heat radiated from the corium pool is also assumed here to be equal to the concrete ablation temperature (1530 K) derived from a threshold volumetric liquid concrete fraction equal to 0.5. The fast oxidation of initial Cr mass is supposed to be achieved at the MCCI onset. The initial corium composition takes into account an early corium splattering of 40 kg above the corium pool by a reduction of the initial corium inventory. The water injection is described, but its impact on the erosion kinetics remains small and is not analyzed below. The concrete composition is obtained from the final report [4] neglecting very minor species and renormalizing the mass fraction of other species. The thermo-chemistry data are evaluated for the mixture of the initial corium inventory with increasing ablated concrete mass with the same method as for CCI2. The ablation enthalpy variation (2.02 MJ/kg) is deduced from GEMINI2 calculations and identical to that used in previous CCI3 interpretation work [11].

### 2.2.2 *Model assumptions*

The solidification temperature determining the pool/upper crust interface temperature is evaluated with the same model as for CCI2. The profile of heat transfer coefficient along the concrete interface is imposed so as to keep the same minimum value of 80 $W/m^2/K$ at the bottom interface and the same maximum value of 300 $W/m^2/K$ at the vertical interface, thus simulating a higher thermal resistance at the bottom interface due to the presence of a crust or solid accumulation. In order to better estimate the observed high corium swelling, the corium void fraction is determined from the Zuber-Findlay correlation multiplied by a factor equal to 1.2.

### 2.2.3 *CCI3 calculation results*

Results are displayed for the axial and lateral ablation kinetics on figure 5, temperature evolution on figure 6 and for the cavity evolution on figure 7.

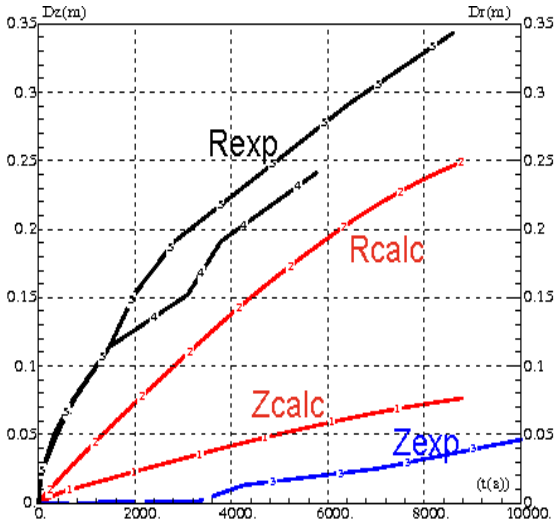


**Figure 5: Lateral (R) and axial (Z) ablation kinetics, comparison of the exp. and calculated values.**

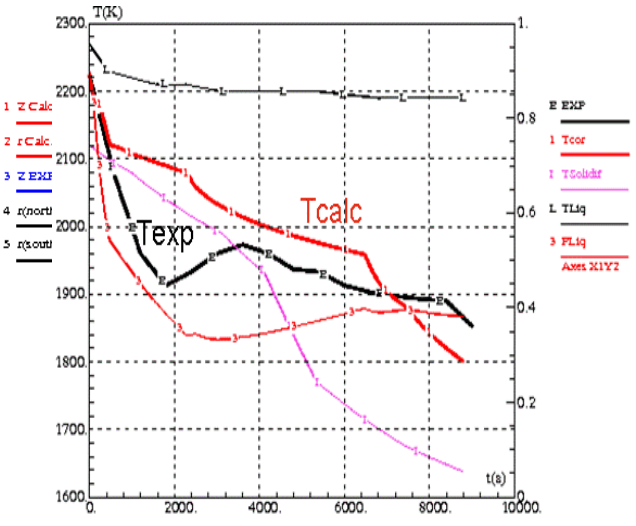


**Figure 6: pool temperature, solidification temp., mass liq. fraction, comparison with measured temperature.**

Concerning the lateral ablation kinetics, the overall agreement between the calculation and the experiment is rather good with some underestimation. However, the axial ablation kinetics is also quite well reproduced by the calculation excepted for a delay for the ablation experimental onset. This delay observed on the experimental ablation onset might be the time needed for the heat diffusion across the crust built-up initially at the bottom, during the experiment, second-rate effect for NPP applications.

The experimental temperature evolution is well reproduced (see figure 5) excepted for the dip in measured temperature, perhaps related to pool non-homogeneities generated in the faster early ablation phase. This good agreement is almost unexpected if reminding that the only link of the interface temperature with the pool corium thermo-chemistry data is the value of the pool/upper crust interface temperature determined from the threshold volume liquid fraction equal to 0.5. In particular

the pool/slag layer interface temperature along the concrete depends only on the hslag heat transfer coefficient and on the concrete ablation temperature.

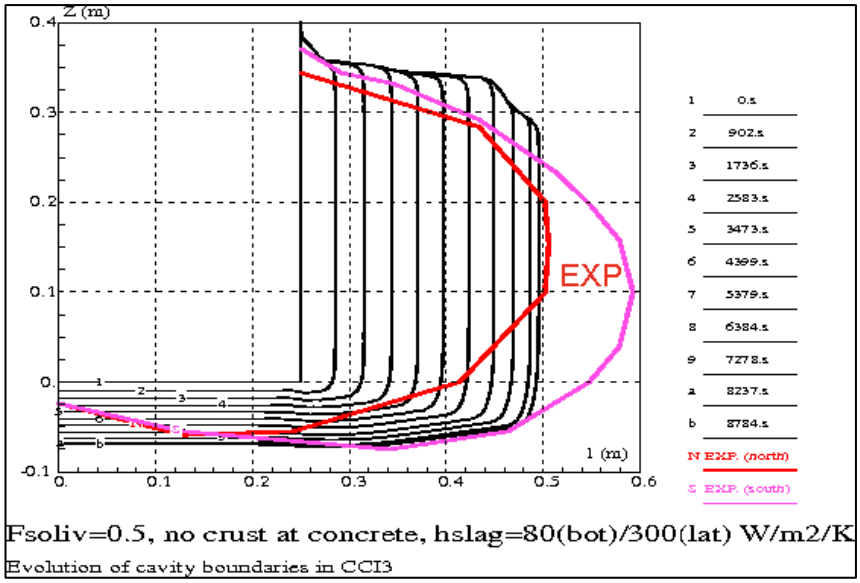


**Figure 7: Cavity evolution and comparison with final experimental data.**

The non uniform profile of slag layer coefficient along the pool interface permits to reproduce very well the very anisotropic ablation (see fig.6). A very good agreement is obtained on the final ablated cavity shape on the south side, and to a less extent on the north side. The calculated final ablated mass (227.7 kg) is also very close to the experimental one (227.5kg) deduced from the final report [4], which shows the overall consistency of the energy balance in calculation compared to the experiment.

## *2.3 Interpretation of CCI5 test*

CCI5 is the largest scale test performed on 2D MCCI in dry conditions: the longest initial pool dimension is indeed equal to 0.79m compared to 0.5m in CCI3 using the same siliceous concrete. Besides the non-ablatable lateral wall on one side permits to investigate the influence of the effective distance between lateral ablatable walls on the gas flow paths through the pool and gas bubbling driven convection pattern.

### *2.3.1 Conditions for the CCI5 test*

The temperature of upper cavity walls is supposed to be equal to the ablation temperature and so identical to that used for CCI3. The oxidation of initial Cr mass is supposed to be achieved at the MCCI onset as for CCI3. The initial corium inventory is obtained from the final report [4] subtracting a splattered mass of 47 kg as recommended [4]. The concrete features are the same as used for CCI3. In order to better estimate the observed high corium swelling, the corium void fraction is determined from the Zuber-Findlay correlation multiplied by factor equal to 1.2 as for CCI3.

### *2.3.2 Model assumptions*

The solidification temperature determining the pool/upper crust interface temperature is evaluated with the same model as for CCI2 and CCI3. The first phase with the prevailing axial ablation might be explained by power injection heterogeneities enhanced at the larger scale. Therefore the profile of the heat transfer coefficient at the concrete interface versus the interface orientation and its evolution versus time (see table 1) are fitted in this first phase to reproduce as well as possible the axial and lateral ablations versus time.

| | First phase (9000s) | Second phase (9000.-17400s) |
|---|---|---|
| **Bottom interface** | 0 < t< 1200s hslag = 100 W/m$^2$/K<br>1200s <t< 1800s: hslag = 1000 W/m$^2$/K<br>1800s < t < 9000s : hslag = 80 W/m$^2$/K | 9000s < t < tend : hslag = 80 W/m$^2$/K |
| **Lateral interface** | 0 <t< 9000s: hslag = 50 W/m$^2$/K | 150 min.<t< tend: hslag = 300 W/m$^2$/K |

**Table 1: Model options and parameters values used for CCI5 test calculations.**

In the later phase beyond 9000s (see figure 8), the lateral ablation prevails on the axial ablation which becomes much slower and more regular; the ablation behaviour becomes similar to that observed in CCI3 test. Therefore the same assumptions as for CCI3 are retained: presence of an inert crust or a solid accumulation at the bottom interface and absence of crust along the lateral concrete interface; the same profile of heat transfer coefficient along the concrete interface (see table 1). Consequently in this second phase, no parameter fitting is performed.

### *2.3.3 CCI5 calculation results*

Because of the unique features of CCI5 test among 2D MCCI with siliceous concrete (large scale, long duration of 5h and first phase with specific axial ablation), more detailed results are displayed for this test to show the overall consistency of calculated results with experimental data. Results obtained are displayed for the axi-lateral ablation kinetics on figure 8, the temperature evolution on figure 9, for the energy balance on figure 10 and the cavity evolution on figure 11.

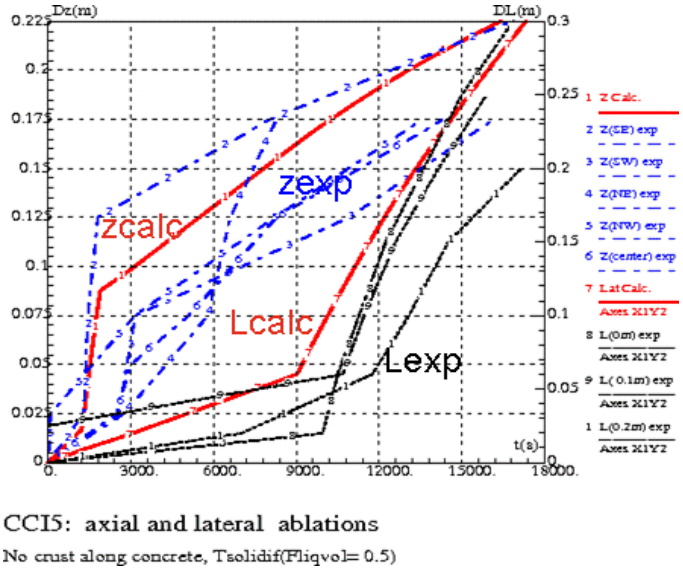


**Figure 8: Lateral (L) and axial (Z) ablation kinetics, comparison with experimental values.**

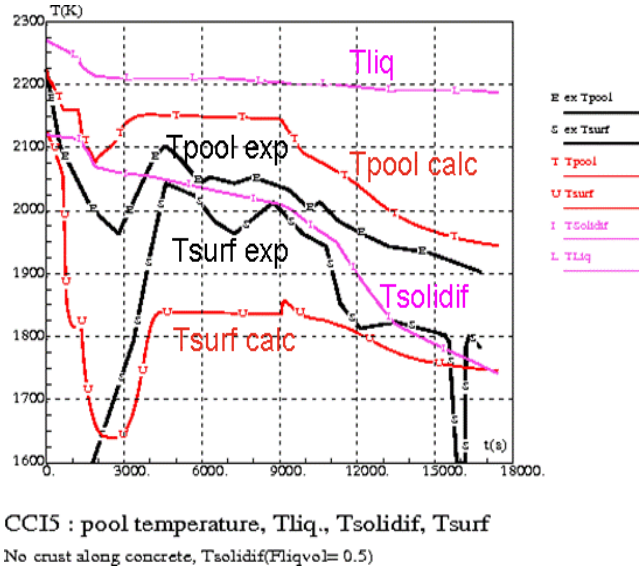


**Figure 9: Pool, liquidus, solidification and surface temperatures, comparison with exp. values.**

The calculation slightly overestimates the pool temperature by only 50 to 100K and the evolution is satisfactory in particular in the second phase. Note that only a low solidification temperature permits to explain that the measured pool temperature stands 200 to 300K below the pool liquidus temperature. The pool upper surface temperature is overestimated by at most 180K in the first phase and then better reproduced in the later phase beyond 12000s. Since the order of magnitude of the upper crust thickness around 1cm or less agrees with the experimental observation, the level of the solidification temperature determining the pool/upper crust interface temperature and influencing strongly this crust thickness should be roughly correct. The discrepancy with the experiment on the surface temperature is more likely related with the possible shielding effect of aerosols released above the pool and the simplistic boundary condition concerning the upper wall temperature (assumed to be equal to 1530K at any time). The comparison of the calculated ablated concrete mass and axi-lateral ablation kinetics with the measured ones and the analysis of the main calculated energy balance terms (see figure 10) permit to check the overall consistency of the results.

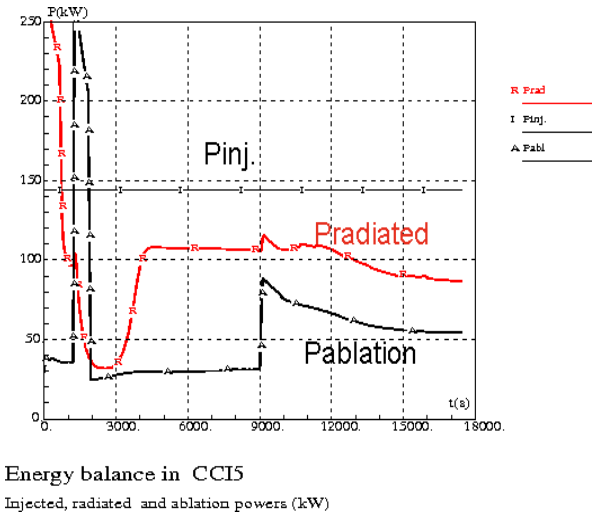


**Figure 10: energy balance in ASTEC/MEDICIS calculation during CCI5 test.**

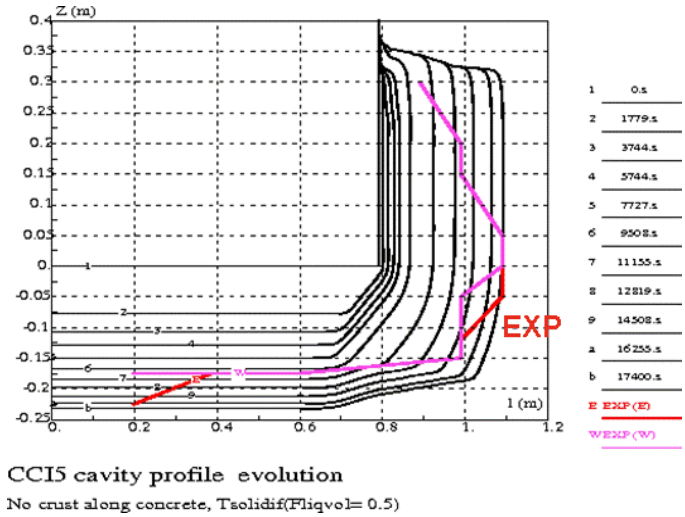


**Figure 11: Cavity evolution in CCI5 with ASTEC/MEDICIS, comparison with final experimental data (EXP).**

The axi-lateral ablation kinetics is correctly reproduced by the calculation in particular in the second phase; the calculated final cavity shape (figure 11) agrees with the experiment excepted for the somewhat overestimated axial ablation and the ablated concrete mass is moderately overestimated by around 19%, 329kg instead of 278kg in the experiment [4].

Thus, the calculated concrete ablation rate and hence the power consumed into ablation agree rather well with the experiment. This also confirms that the calculated upwards radiated power (see figure 10), which corresponds to around 70% of the injected power and impacts strongly on the ablation rate, is surely reasonably evaluated. Indeed, the power consumed into concrete ablation is only around 34% (see figure 10) and a reduction of only 10% on the radiated power will increase the power consumed into ablation and then the ablated concrete mass by at least 20%. The high level of radiated power is due to the large upper pool interface area compared to the area of concrete interfaces and is still enhanced by the low pool/upper crust interface temperature or equivalently the low solidification temperature.

To be complete, this analysis must include the concrete conduction losses and the corium thermal energy variation. The contribution of lost power by conduction behind the final front ablation evaluated by a simple analytical model assuming a quasi-state situation with a constant ablation rate (see details in the paragraph 3) amounts only to 6.8% of the injected power and is ignored here. The discrepancy between calculated and measured temperatures generates a difference in the corium thermal storage variation rate corresponding to only around 3% of the injected power. Taking into account the conduction loss power and the difference in corium thermal energy storage in the energy balance will contribute to reduce slightly the effective injected power and the concrete ablated mass but this will not change the above analysis.

Finally, the CCI5 test, which is the largest scale 2D MCCI experiment in dry conditions, was recalculated satisfactorily using a set of simple assumptions and models for the interface structure without any parameter fitting for the later phase and with a consistent energy balance permitted by the detailed fitting in the first phase.

# 3 Interpretation of VULCANO experiments

## *3.1 VBU5 test*

As detailed in the previous chapter, the new approach mainly based on the assumption of the formation of a mushy boundary layer without a stable crust at the pool/concrete interface is kept here to analyse VULCANO experiments.

### *3.1.1 Test features and assumptions*

VBU5 test [5,6] is very similar to CCI3 test regarding the concrete composition, i.e. siliceous concrete. The initial corium composition is quite different as its refractory oxides fraction is higher compared to that of CCI3 (92% versus 77%). The VBU5 corium pool is a half-cylindrical geometry (diameter 30 cm), and closed by a porous zirconia plate. Since this configuration is not described by MEDICIS, a cylindrical geometry is assumed doubling corium masses and experimental injected power. Due to the heating technology (RF heating), thermal losses in the alumina plate are significant and have thus to be taken into account in the simulation for the total injected power.

Similar assumptions to those used for CCI3 test are retained for VBU5 test due to similar features and to make easier the comparison between the results obtained on both experiments, so the profile of heat transfer coefficient along the interface is identical. Based on GEMINI2 data, ablation temperature is set to 1470K, and enthalpy variation ($\Delta H$) to 1.92 MJ/kg. The solidification temperature determining the pool/upper crust interface temperature is evaluated from a volumetric liquid fraction equal to 0.3 (best fit).

However two main differences have to be noted. Firstly, due to the VULCANO open cavity geometry, temperature of upper walls receiving the power radiated from the corium pool is assumed to be at room temperature. Secondly, compared to CCIX experiments, the VULCANO geometry combined with a quite short test duration lead to a higher fraction of power lost by conduction into the concrete section beyond the ablation front. As no specific model of conduction into concrete is implemented in the MEDICIS code, a simplified model, recently proposed by Tourniaire et al. [12] and assuming a quasi-state regime, is used to evaluate an average value of energy lost by conduction during a VULCANO experiment and thus impacting the injected power. Thermo-chemistry data are evaluated for the mixture of the initial corium inventory with increasing ablated concrete mass using once again the interface with GEMINI2 solver and the NUCLEA database [8].

### *3.1.2 VBU5 calculation results*

Conduction losses into concrete are estimated here to 4.65 kW. Only the thermal losses through the radial interface are considered here since the characteristic time required for reaching the steady state regime for the axial interface is too high compared to the test duration, so it is not relevant. Moreover, it is assumed that thermal losses are significant only during the initial transient and also later as the instantaneous ablation velocity becomes lower than the average ablation velocity. In a first approximation, the first fraction is neglected, thus the power lost by conduction is restricted to the long-term phase of the test, as displayed by the figure 12. Obviously this distribution impacts directly the injected net power profile for the ASTEC/MEDICIS calculation.

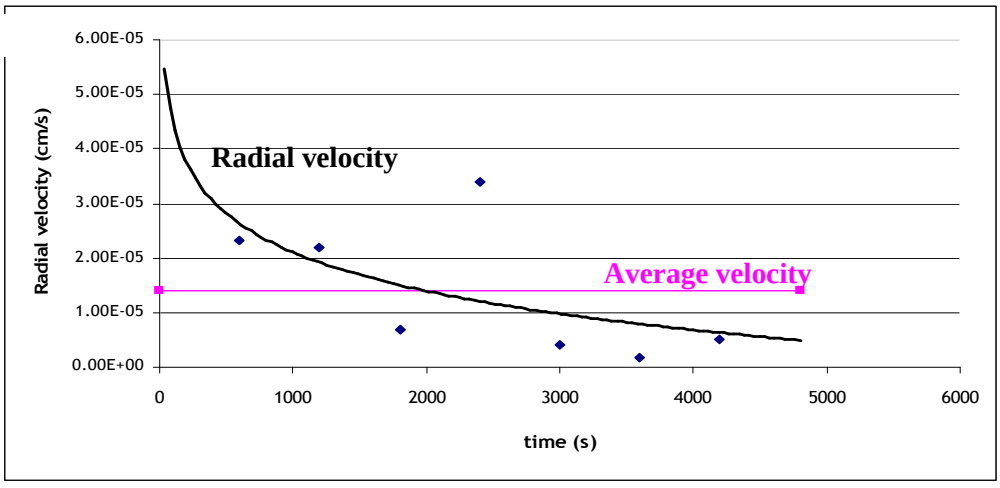


**Figure 12: Instantaneous and average radial velocities as a function of time.**

This set of assumptions leads to a rather good agreement between axial and radial ablation kinetics and the related experimental data (see figure. 13). The comparison of the final cavity shape

calculated and the experimental one is also quite satisfactorily (see figure. 14). During the calculation the upper crust thickness is close to the experimental value i.e. 2 or 3 cm, indicating that the calculated radiated power should be correct in spite of the absence of relevant surface temperature measurements. Finally, the total ablated concrete volume is also well simulated since we obtain 17.1 L compared to the experimental value of 17.3 L.

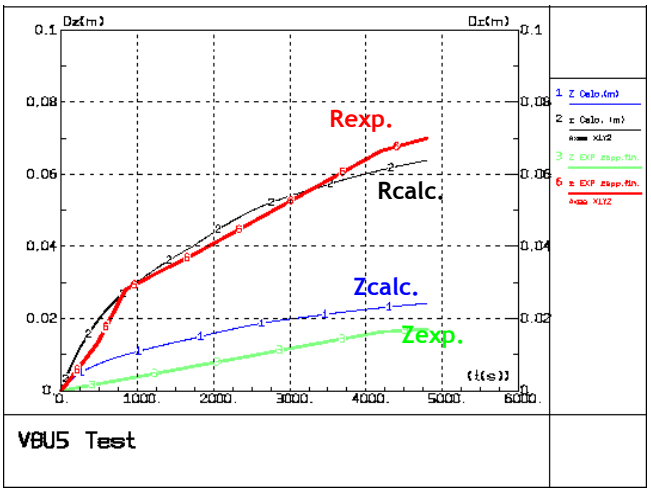


**Figure 13: Lateral and axial ablation kinetics, comparison with experimental values (FSOLIDIV=0.3).**

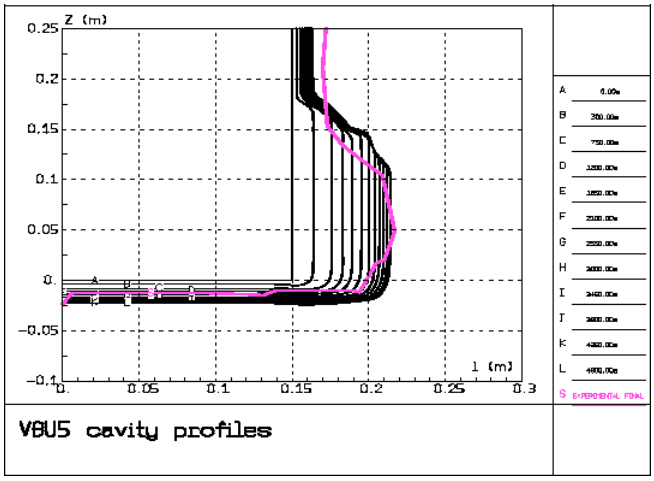


**Figure 14: Cavity boundaries evolution, comparison with exp. Data (FSOLIDIV=0.3).**

The evolution of the corium temperature is compared to the experimental data (black curve) on figure 15. The experimental temperature evolution is badly reproduced by ASTEC/MEDICIS, as the calculated corium temperature decreases very fast after the beginning of the corium concrete interaction. However, for this test only one measurement at 1200 s is available, and a very bad confidence is given to this value, preventing thus any conclusion on the effective experimental temperature evolution.

An additional calculation was performed, based on the assumptions used in the former approach presented in the last seminar in 2007, i.e. existence of a crust at all interfaces. In this case, the solidification temperature is determined by a γ value of 0.2. The results, displayed on figure 16, indicates that even if a quite high solidification threshold is used, the measured corium temperature cannot be well simulated and above all an over-estimation of the final ablated volume (near 20%) is obtained, leading thus to an incorrect energy balance. Some hypotheses to explain the behaviour of the pool temperature are presented in the discussion paragraph.

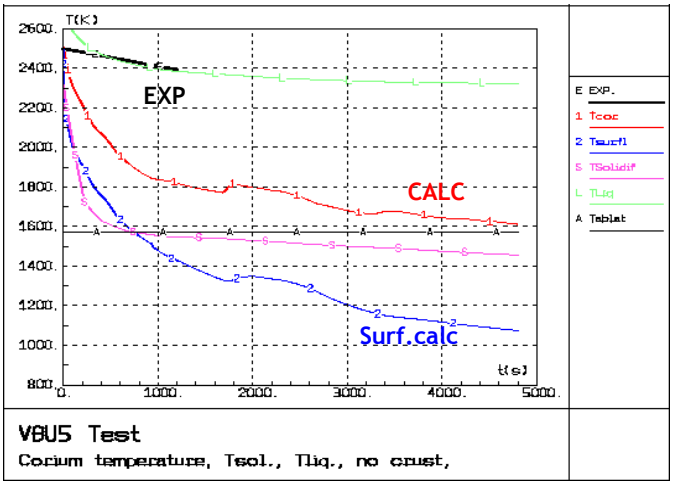


**Figure 15: Temperature evolutions, comparison of the experimental and calculated values (FSOLIDIV=0.3).**

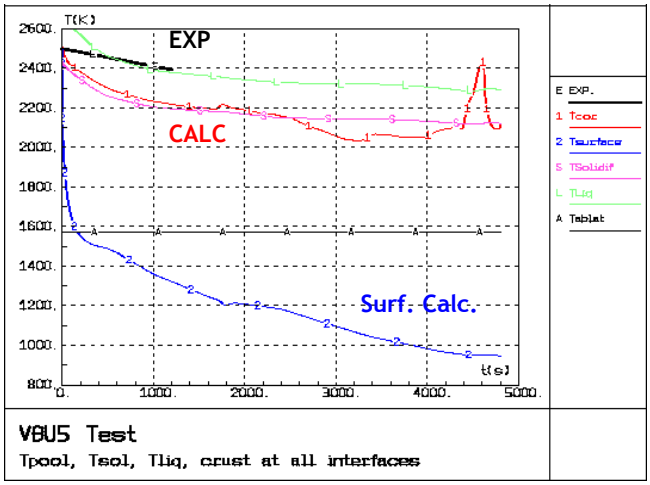


**Figure 16: Temperature evolutions, comparison of the experimental and calculated values (γ=0.2).**

### 3.2 VBES-U2 test

This test is quite specific as it belongs to the "separate effects tests program" [13]. Indeed, for this more analytical test it was used a cement clinker-based concrete rich in calcium oxide but very poor in carbon dioxide in order to assess the effect of the physico-chemical concrete features and more particularly the effect of the components granulometry and aggregates behaviour at the ablation temperature, which was highly suspected to explain the ablation dissymmetry in the case of siliceous concretes [15].

#### 3.2.1 Test features and assumptions

The general conditions of VBES-U2 test are deduced from the experimental reports [14, 15]. As it was said, CaCO3 aggregates were replaced by clinker aggregates, so this particular concrete has exactly the same properties of a limestone concrete in terms of viscosity, liquidus and solidus temperatures, except the presence of aggregates remaining at ablation temperature like for siliceous concrete. It is mentioned that even if the carbon dioxide fraction is equal to zero, the total gas molar fraction remains significant due to the relative high fraction of water needed by the clinker concrete processing. The value of the ablation temperature is 1530K and of the ablation enthalpy variation is 1.79 MJ/kg. The pool geometry is the same as that of VBU5 as well as the initial corium composition.

Identical assumptions to those used for VBU5 test are retained in terms of slag layer heat transfer coefficients profile, upward structures temperature, viscosity model, conduction losses into concrete… The volumetric liquid fraction used to evaluate the solidification temperature is equal to 0.5.

#### 3.2.2 VBES-U2 calculation results

In this case conduction losses into concrete are estimated to 9.1 kW. In the same way as VBU5 test, the power lost by conduction is shifted to the long-term phase of the VBESU2 test, i.e. after 4500 seconds.

Results are displayed on figure 17 for cavity evolution, on figure 18 for the axial and lateral ablation kinetics, and on figure 19 for the temperature evolution. The overall energy balance seems to be relevant, as the results of kinetics and total ablated concrete volume are consistent with the experimental data. The calculated upper crust thickness is also in accordance with the experimental observations.

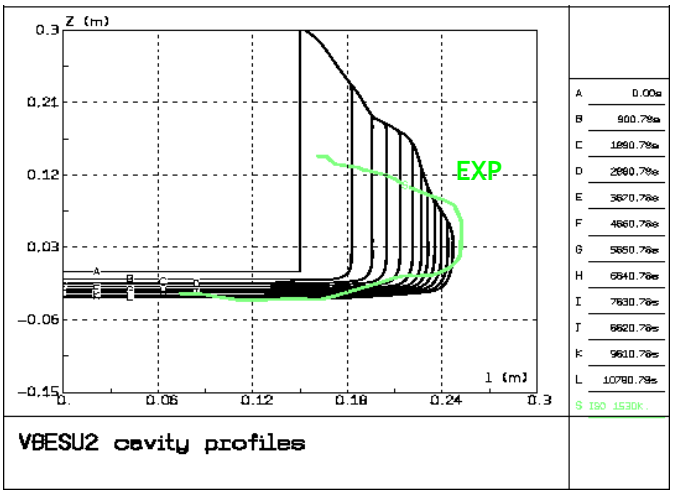


**Figure 17: Cavity boundaries evolution (FSOLIDIV=0.5), comparison with exp. data (EXP).**

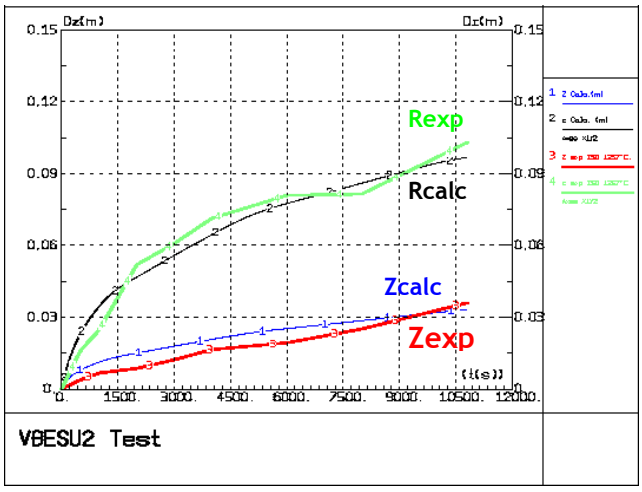


**Figure 18: Lateral (R) and axial (L) ablation kinetics, comparison with exp. values (FSOLIDIV=0.5).**

Contrary to VBU5 test, surface temperatures could be measured here with accuracy so the experimental radiation power can be deduced from the following expression:

$$P_{rad} = \sigma . \frac{1}{\frac{1}{\varepsilon_1} + \frac{1}{\varepsilon_2} - 1} . \left( T_{surface}^4 - T_{environment}^4 \right) . S$$

with ε1=ε2=0.8 and S= $\pi R^2_{cavity}(t)$

The figure 20 presents the comparison between calculated and experimental radiation powers. The overestimation is due to an upper crust thickness slightly underestimated during the first part of the test. After 5000s. a saturation of the pyrometer occurs leading thus to an overestimation of the experimental value.

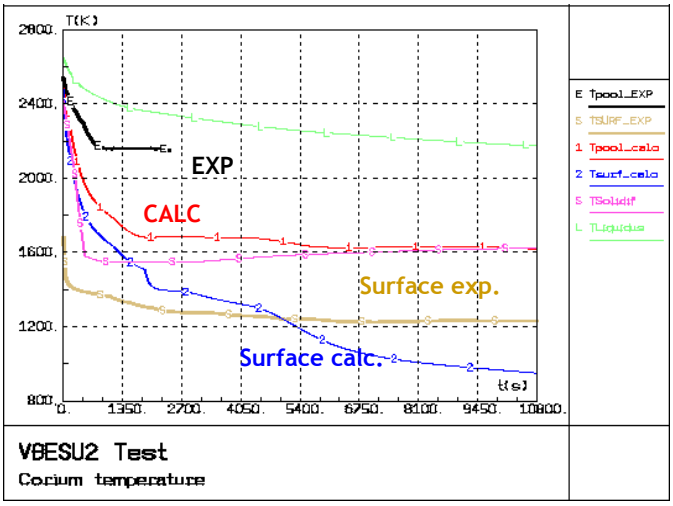


**Figure 19: Temperature evolutions, comparison with the experimental values (FSOLIDIV=0.45).**

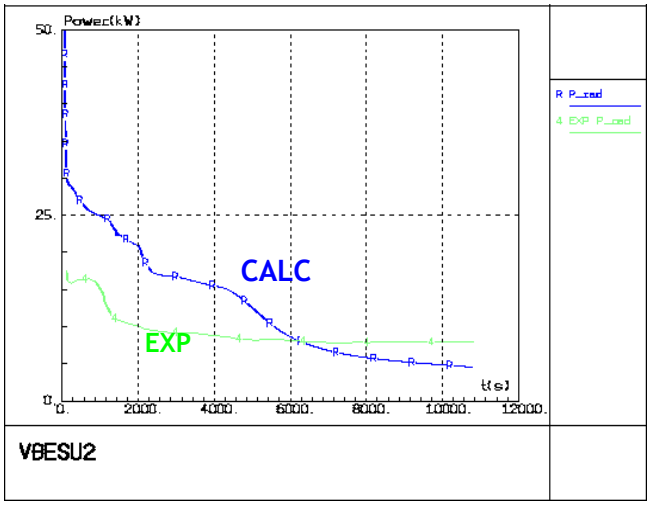


**Figure 20: Comparison of calculated and experimental radiation powers.**

Once again, since the pool temperature decrease is overestimated, another calculation was performed using a low γ value (0.25). The corium pool temperature evolution, displayed on figure 21, confirms that the experimental temperature can not be well simulated without an over-estimation of the final ablated volume, near 100% (see figure 22). Besides the volume parameter, the final cavity shape cannot be well reproduced with this set of assumptions as the ablation dissymmetry is limited by the presence of a crust all along the interfaces thus preventing the effect of the imposed hslag profile. The upper crust thickness evolution is also not consistent with the experimental observations as more than 7cm. compared to 3cm in the test are calculated during the first 5000 s.

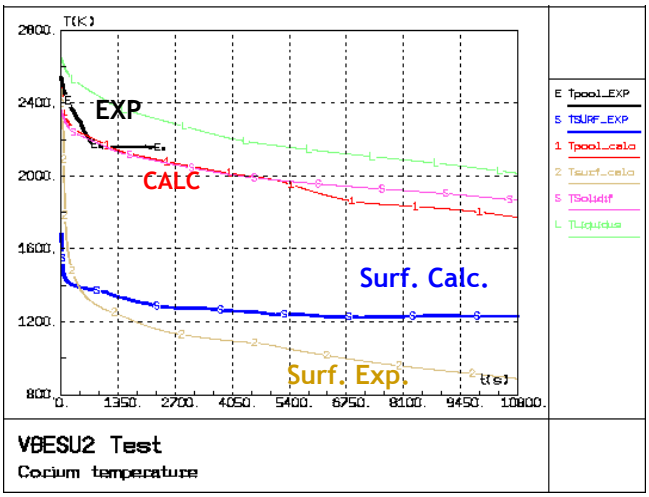


**Figure 21: Temperature evolutions, comparison with the experimental values (γ=0.25).**

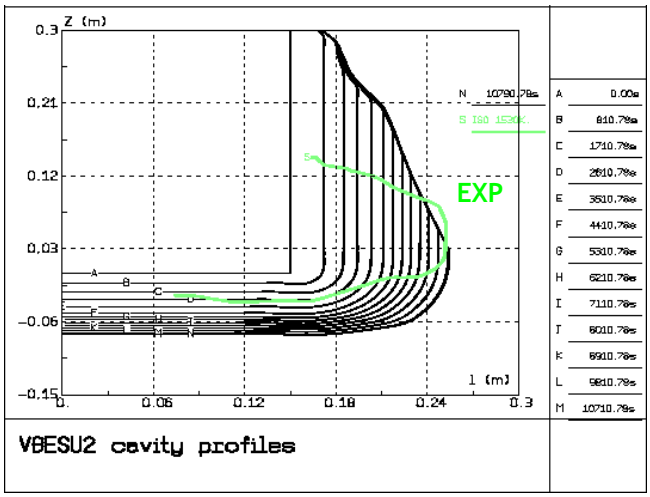


**Figure 22: Lateral and axial ablation kinetics, comparison with exp. values (γ=0.25).**

Finally, assuming that clinker aggregates may not be dissolved directly in the corium pool and leading thus to a higher global pool viscosity, a last calculation was performed using the options on the viscosity correlation in order to reduce the rapid pool temperature decrease. It is recalled that in MEDICIS the viscosity is a function of the pool composition, pool temperature, and the volumetric solid fraction according to: $\mu(y,T,f_{vs}) = \mu_{liq}(y,T).\mu_r(f_{vs})$ with:

$$\mu_r = \left( 1 + \frac{0{,}75 \, f_{vs} / f_{vs\max}}{1 - f_{vs} / f_{vs\max}} \right)^2$$

$fvs_{max} = 1 - fliq_{min}$
$fliq_{min}$= 0.35 according to Stedman et al. [16].

A sensitivity study was performed onto $fliq_{min}$ parameter, corresponding to the threshold value inducing an infinite viscosity. Results show that using high values of $fliq_{min}$ [0.5; 0.75] (certainly not representative), the experimental decrease temperature is well reproduced; nevertheless the overall energy balance deviates too far from experimental data. Some alternative hypotheses to explain the behaviour of the corium pool temperature are presented in the next Discussion paragraph.

# 4 Discussion

The good agreement obtained between calculation and experiment on CCIX tests and on VBU5 and VBES-U2 tests for the axi-radial ablation kinetics and the final cavity shape and ablated concrete mass (or total ablated volume) shows basically the relevance of the set of assumptions and models used above. The pool temperature evolution is also well reproduced in CCIX tests but the temperature decrease rate is overestimated by recalculations in VBU5 test and still more in the VBESU2 test. No convincing explanation related to model limitations is found for this discrepancy: the use of an alternative pool/concrete interface structure assuming the presence of a crust and a higher solidification temperature permits to get a good prediction of the temperature evolution but at the expense of a largely overestimated ablated concrete volume. Two other assumptions are proposed here to explain the rapid decrease of the pool temperature in VULCANO calculations:

1) the release of light refractory clinker aggregates from the lateral interface leads to their accumulation at the top of the pool hindering their mixing in the pool and thus reduces the pool temperature decrease. PTE of VBES-U2 will be useful to verify if some CaO particles can be clearly identified as segregated phases in the bulk pool.

2) based on axi-radial kinetics, it is likely that the in-flux of aggregates released from the bottom interface is low and moreover this small released fraction will accumulate under the solid accumulation and thus will be mixed into pool with delay, thus the measured temperature through W thermocouples located at the bottom can be locally overestimated, and obviously not representative of the average bulk temperature.

Finally, another assumption can be pointed out to explain the different bulk temperature behaviours between CCI and VULCANO experiments. Indeed, if one look at the corium properties, it appears that CCIX tests initial corium inventories are less refractory than those of VULCANO tests, which is confirmed by the initial measured bulk temperatures; nevertheless the experimental bulk temperature decrease is higher for VULCANO tests (during the first 2400 s.). As a conclusion, it can be said that CCIX bulk pools are less sensitivity to lighter oxides enrichment coming from the concrete. Two combined explanations are proposed herafter:

a) the S/V ratio is significantly different for each test section : $S/V_{(VULCANO)}$= 17.4 $m^{-1}$ and $S/V_{(CCI)}$= 5.55 $m^{-1}$. This means that for the same ablated concrete mass, the decrease of high oxides fraction (HOF) is lower for CCI tests. It is mentioned that HOF boundaries are equal to [0.77; 0.46] for CCI3, [0.91; 0.54] for VBU5 and [0.92; 0.51] for VBES-U2 (see comments on figure 23);

b) in addition, the thermo-chemical properties of the corium-concrete mixes are different according to the type of the experiments. Figure 23 displays for example the solidification temperature as a function of the high oxides fraction (HOF), based on a volumetric solid fraction equal to 50%. It appears clearly that the solidification temperature decrease kinetics as a function of light oxides enrichment in the bulk is slower in the case of CCI3 test compared to VBU5 test and still more to VBES-U2 test and so less sensitive to any error on the effective bulk pool composition in case of aggregate segregation.

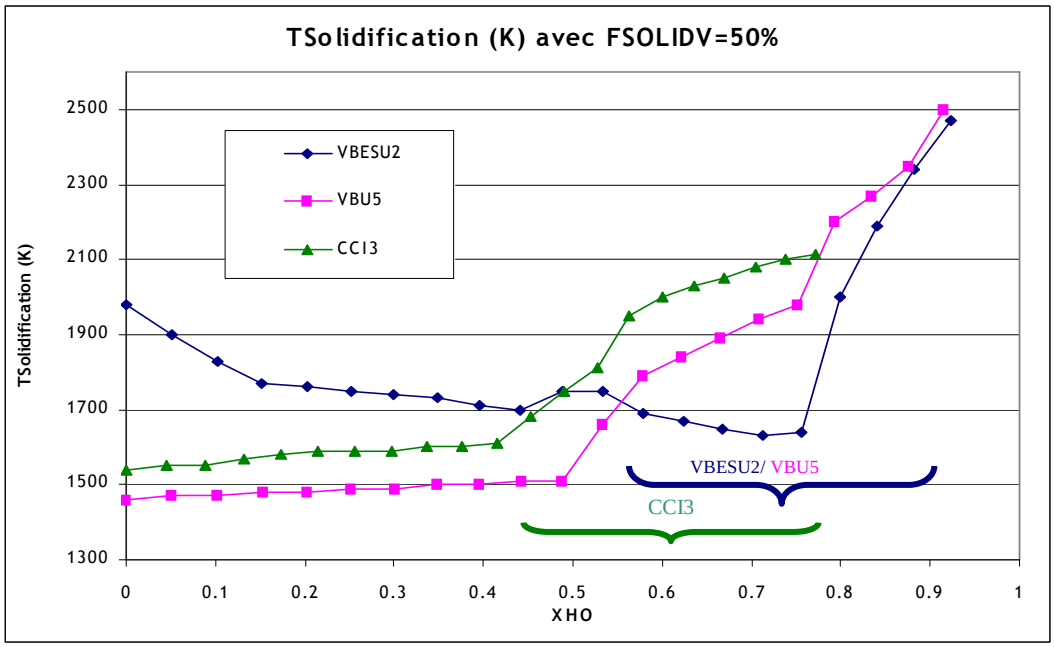


**Figure 23: Solidification temperature as a function of the high oxides fraction (HOF).**

The proposed interface structure model has strong implications for the predicted axi-radial ablation kinetics in the reactor case as shown elsewhere [17]. It is then worthwhile looking at the physical meaning of this interface structure model even if it appears at first view oversimplified and too approximate. This model assumes the absence of any stable crust along the lateral oxidic corium/concrete interface for all concrete type and along all concrete interfaces in case of LCS concrete. In the absence of crust, the thermal resistance of the interface might be determined by that of a thin boundary layer, corresponding to the zone of mixing of concrete oxides with corium and around 3 mm thick, thus leading to the assumed heat transfer coefficient value of around 300 $W/m^2/K$.

Direct numerical simulation work performed recently at IRSN [18] might help confirming and completing the description of the concrete/corium mixing boundary layer and of the structure of concrete plumes at the interface vicinity. The same result can be obtained assuming the presence of a 1cm thick inert crust (without link with a solidification temperature) but the stability of such a crust along the lateral interface is unlikely at least for mechanical reasons. The reduced thermal resistance of the bottom interface is determined by that of a solid accumulation. This accumulation might be the initial refractory crust built-up at first corium/concrete contact, then fed by the settling of crust remnants, released from lateral interface or generated by the cooling due to aggregates released from the same interface, and also by aggregates released at the bottom interface and piled-up below the initial crust. The assumed heat transfer coefficient value of around 80 $W/m^2/K$ corresponds to a porous solid thickness of 2.5 to 4cm according to its porosity.

The main limitation of the MCCI knowledge presented here is the use of parametric models whose application to the reactor case at large scale and in the long term might be questionable. However the basic underlying assumptions, i.e. the absence of crust along the lateral oxidic corium/concrete interface and the build-up of the upper crust at a solidification temperature determined by a volumetric liquid fraction were shown to be promising when applied to the 2D MCCI experimental database. It is recalled here that an only 3cm thick stable solid accumulation is sufficient to generate a large ablation anisotropy. Such a thin solid accumulation will not melt in the reactor case even if taking into account the decay power released into it. The most uncertain point is the long term behaviour of the initially built-up crust or solid accumulation at the bottom interface in case of siliceous concrete. This question should be answered by building more mechanistic models on the initial formation of this bottom crust or solid accumulation, its evolution and its possible dissolution. Such a model should also explain why no solid accumulation appears clearly at the bottom in case of LCS concrete: the reason might be the less refractory nature of the corium/LCS concrete mixture promoting the dissolution of the solid accumulation. However this explanation is not supported by results of VBES-U2 test where the mixture of corium with clinker concrete is also less refractory than pure concrete (see figure 23) but which shows an increased thermal resistance at the bottom and hence a solid accumulation or crust stable at least during the rather short duration of the VBESU2 experiment. This points out nevertheless that the difference in MCCI behaviour between CCI2 and VBES-U2 tests is likely to be related to the intact aggregate accumulation built-up at the bottom interface in case of VBES-U2 and not in case of CCI2 where aggregates are already destroyed at ablation.

# 5 Conclusions

Most of 2D MCCI experiments with real material in a homogeneous oxidic pool configuration have been analysed and interpreted with the help of the ASTEC/MEDICIS code. Main findings obtained from these experiments concern the 2D heat transfer towards pool interfaces during MCCI and indirectly the structure of the pool/concrete interface.

Our present interpretation assumes the absence of stable crust along the lateral oxidic corium/concrete interface for any concrete type and along all concrete interfaces in case of LCS concrete. The rather thin upper crust is an indication of the low solidification temperature permitting the formation of this crust, which can be evaluated using precise thermo-chemistry data from the corium mobility threshold temperature corresponding to a volume liquid fraction near 0.5.

In the case of limestone-sand concrete (CCI2 experiment), the explanation of the almost uniform ablation is straightforward if assuming the pool/concrete interface is the same whatever the orientation. One possible reason is that no solid accumulation appears at the bottom or at least is dissolved very rapidly due to the low refractory nature of the corium crust/concrete mixture.

In the case of concrete with aggregates remaining intact during ablation (CCI3, CCI5, VBU5, and VBES-U2 experiments), the prevailing lateral ablation cannot be related to a possible anisotropy of convective heat transfer within the bulk pool where convective heat transfer is very efficient ; it is explained rather by the dissymmetry between higher bottom and lateral interface thermal resistances. At the bottom interface, a stable solid accumulation fed by the initial crust formation and the settling of refractory material crust fragments enhanced by the cooling due to aggregates released from the lateral interface, builds-up and imposes a high downwards thermal resistance. Along the lateral interface, the absence of solid accumulation or stable crust explains the lower thermal resistance compared to the bottom one. These assumptions permit to reproduce rather satisfactorily the axi-radial ablation kinetics in all experiments.

The main unsolved issue concerning the 2D ablation in an homogeneous pool is the long term behaviour of the solid accumulation or crust possibly built-up at the cavity bottom very early during MCCI in particular in case of a siliceous concrete. There is clearly a need to build a more mechanistic model, taking into account in particular the aggregates behaviour at ablation threshold to predict the evolution of the solid accumulation at the cavity bottom in the reactor case in the long term phase i.e. after around 10 hours.

## References


1) M. Cranga, C. Mun, B. Michel, F. Duval, M. Barrachin, Status of the interpretation of the real material 2D MCCI experiments, MCCI-OECD seminar, Cadarache, St-Paul lez Durance, France, October, 2007.
2) M. T. Farmer, S. Lomperski, S. Basu, A summary of findings from the melt coolability and concrete interaction (MCCI) program , Proceedings of ICAPP07, Nice, France, May 13-18th 2007.
3) M. Farmer et al, OECD-MCCI project: 2-D Concrete Interaction (CCI) Tests, Final report, OECD-MCCI -2005-TR05, February 28th 2006.
4) M. Farmer et al, OECD-MCCI project : Category tests to Generate Core Concrete Interaction data, Final report, OECD-MCCI -2010-TR06, August 2010
5) C. Journeau et al, Behaviour of nuclear reactor pit concretes under severe accident conditions", Proc. CONSEC '07, Concrete under Severe Conditions, Tours, France (2007).
6) C. Journeau, P. Piluso, , J.F. Haquet, E. Boccaccio, V. Saldo, J-Michel Bonnet, S. Malaval, L. Carénini, L. Brissonneau, Two-dimensional interaction of oxidic corium with concretes: The VULCANO VB Test Series, Annals of Nuclear Energy, 36, pp.1597-1613, 2009.
7) M. Cranga, R. Fabianelli, F. Jacq, M. Barrachin, F. Duval, The MEDICIS code, a versatile tool for MCCI modelling, Proceedings of ICAPP05, Seoul, Korea, May 15-19th 2005.
8) B. Cheynet, P. Chaud, PY. Chevalier, E. Fischer, P. Mason, M. Mignanelli, NUCLEA "propriétés - dynamiques et équilibres de phases dans les systèmes d'intérêt nucléaire". In: Journal de Physique IV - France, 113, 61-64, 2004.
9) J.M.Bonnet, Thermal hydraulic phenomena in corium pools for ex-vessel situations: the BALI experiment, Proceedings of ICONE8, 8th Int. Conf. on Nuclear Engineering, April 2-6, 2000, Baltimore, USA.
10) B. Spindler et al, Simulation of Molten Corium Concrete Interaction: the benchmark: the CCI2 Benchmark organized in the frame of the OECD-MCCI project, June 2007.
11) M. Cranga, C. Mun, B. Michel, F. Duval, M. Barrachin, Interpretation of real material 2D MCCI experiments in homogeneous oxidic pool with the ASTEC/MEDICIS code, Proceedings of ICAPP08, Anaheim, California, June 8-12th 2008.
12) B. Tourniaire, B. Spindler, M. Guillaumé, Transient conduction heat transfer modelling in concrete for the simulation of long term phase of molten core concrete interaction, Proceedings of ICAPP08, Anaheim, California, June 8-12th 2008.
13) C. Journeau et al, Separate Effect Tests with Artificial Concretes to Determine the Causes of Ablation Anisotropy, MCCI-OECD seminar, Cadarache, St-Paul-lez-Durance, France, November 15-17th 2010.
14) C.Journeau, L.Ferry, Presentation of the VULCANO VB-ES-U2 test, report SARNET2-MCCI-P01, 2009.
15) L. Ferry, M. Breton, J. Monerris, Y. Bullado, F. Compagnon, G. Fritz, P. Correggio, Interaction corium-béton en bain tout oxyde sur l'installation VULCANO: essai a effets séparés VBES-U2 (Béton à base de clinker), NT DEN/DTN/STRI/LMA/2009/024, 2009.
16) S. Stedman, J. Evans, J., Woodthorpe, Rheology of Composite Ceramic Injection Moulding. Suspensions. Journal of Material Science 25, 1833–1841, 1990.
17) M. Cranga, B. Michel, C. Mun, M. Barrachin, Outcome of the available 2D MCCI experimental database for the reactor case in dry conditions, MCCI-OECD seminar, Cadarache, St-Paul lez Durance, France, November 15-17th 2010.
18) C. Introïni, Interaction entre un fluide à haute température et un béton : contribution à la modélisation des échanges de masse et de chaleur'', Thèse de l'Ecole Doctorale Mécanique Energétique Génie Civil Procédés ED n°468, Institut National Polytechnique de Toulouse (2010) in press.